

## COMPARISON OF THE THERMAL DEGRADATION MECHANISM OF $\text{Li}_x(\text{Ni},\text{M})\text{O}_2$ SYSTEMS (M = Al, Co/Al, Mn, x = 0.50, 0.30)

M. Guilmard<sup>a</sup>, L. Croguennec<sup>a</sup>, G. Rousse<sup>b</sup>, F. Fauth<sup>c</sup>, C. Jordy<sup>d</sup>, Ph. Biensan<sup>d</sup> and C. Delmas<sup>a</sup>

<sup>a</sup> Institut de Chimie de la Matière Condensée de Bordeaux-CNRS and Ecole Nationale Supérieure de Chimie et Physique de Bordeaux, Université Bordeaux I, 87, Av. du Dr. A. Schweitzer, 33608 Pessac Cedex (France)

<sup>b</sup> Institut Laue Langevin, BP 156, 38042 Grenoble Cedex 9 (France)

<sup>c</sup> European Synchrotron Radiation Facility (ESRF), BP 220, 6, rue Jules Horowitz, 38043 Grenoble (France)

<sup>d</sup> SAFT, Direction de la recherche, 111 Bd. Alfred Daney, 33074 Bordeaux Cedex (France)

Lithium nickelate is one of the most attractive materials for lithium ion batteries due to its high capacity and low cost. Nevertheless, the fully charged  $\text{LiNiO}_2$  is unstable at high temperature. This instability leads to oxygen release, which can react with the organic solvents of the electrolyte in an exothermic reaction. Differential Scanning Calorimetry (DSC) measurements have shown the positive effect of partial aluminum or manganese substitutions on the thermal stabilization of the structure [1-3].

The thermal degradation mechanism of the  $\text{Li}_x(\text{Ni},\text{M})\text{O}_2$  (M = Al, Co/Al, Mn, x = 0.50, 0.30) deintercalated phases was studied by Thermal Gravimetric Analyses coupled with Mass Spectrometry. Correlation with *in situ* X-ray and neutron diffraction experiments was then achieved to determine the degradation mechanism and to explain the differences in thermal stability observed depending on the material composition. A similar degradation mechanism is observed for the four types of materials ( $\text{Li}_x\text{Ni}_{1.02}\text{O}_2$ ,  $\text{Li}_x\text{Ni}_{0.89}\text{Al}_{0.16}\text{O}_2$ ,  $\text{Li}_x\text{Ni}_{0.70}\text{Co}_{0.15}\text{Al}_{0.15}\text{O}_2$  and  $\text{Li}_x\text{Ni}_{0.90}\text{Mn}_{0.10}\text{O}_2$ ). As clearly observed in Fig. 1 on the enlargement of the *in situ* neutron diffraction patterns of  $\text{Li}_{0.30}\text{Ni}_{0.89}\text{Al}_{0.16}\text{O}_2$  represented, it occurs in two steps:

- the first one, corresponding to the structural transition between the initial lamellar  $\alpha$ - $\text{NaFeO}_2$ -type phase (R-3m) and a “ $\text{LiM}_2\text{O}_4$ ” pseudo-spinel-type phase (Fd3m), is associated with an oxygen release only for a lithium content smaller than 0.50,

- the second one corresponds to the transition between the “ $\text{LiM}_2\text{O}_4$ ” pseudo-spinel-type phase (Fd3m) and a NiO-type phase (Fm3m), through the formation of a highly disordered R-3m phase. This second step is associated with an oxygen release whatever the lithium content.

Influence of the substituant nature is then discussed. It appears that an increasing aluminum substitution for nickel induces slower kinetics for the various phase transitions (Fig. 2). Cobalt substitution improves the stability of the initial  $\text{Li}_x(\text{Ni},\text{Al})\text{O}_2$  material by rising up the temperature of the pseudo-spinel formation. Manganese substitution appears to stabilize the pseudo-spinel phase, as this phase disappears at a higher temperature than the pseudo-spinel phase corresponding to  $\text{Li}_x\text{Ni}_{1.02}\text{O}_2$ .

### References

- [1] T. Ohzuku, T. Yanagawa, M. Kouguchi and A. Ueda, J. Power Sources 68(1) (1997) 131.  
[2] H. Arai, S. Okada, Y. Sakurai and J. Yamaki,

J. Electrochem. Soc. 144(9) (1997) 3117.

- [3] P. Biensan, B. Simon, J. P. Pérès, A. De Guibert, M. Broussely, J. M. Bodet and F. Pertion, J. Power Sources 81-82 (1999) 906.

### Acknowledgements

The authors thank P. Dagault and D. Denux for thermal analyses, SAFT and Région Aquitaine for financial support.

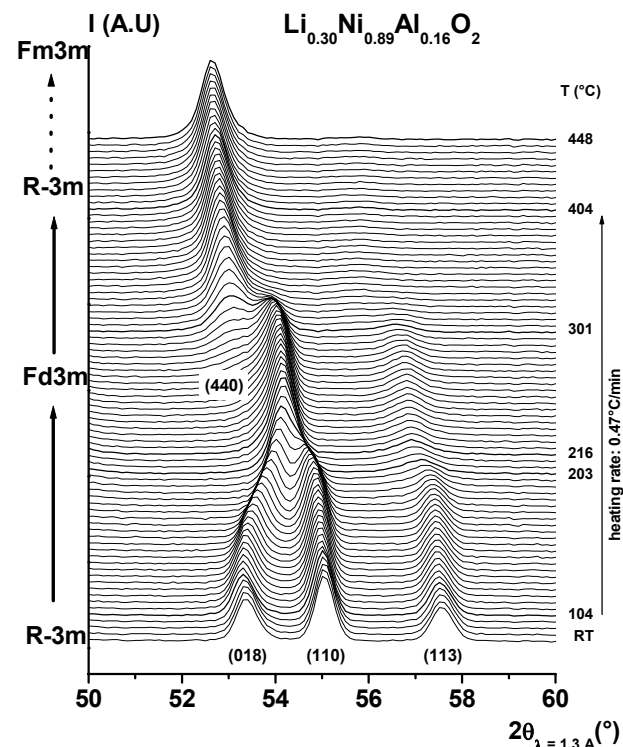


Fig. 1: Enlargement of the *in situ* neutron diffraction patterns of  $\text{Li}_{0.30}\text{Ni}_{0.89}\text{Al}_{0.16}\text{O}_2$ , upon increasing temperature, in the  $[50 - 60^\circ (2\theta)]$  range (heating rate:  $0.47^\circ\text{C}/\text{min}$ , acquisition time: 10 min).

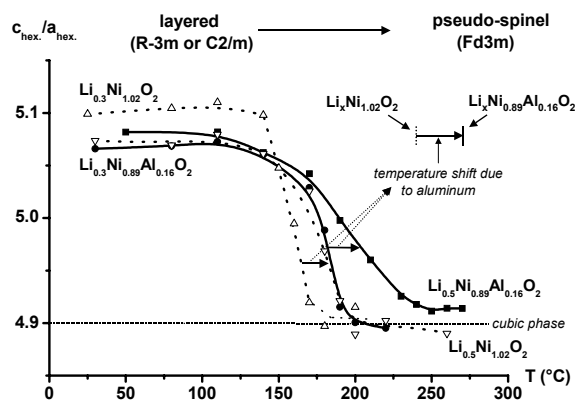


Fig. 2: Evolution of the  $c_{\text{hex}}/a_{\text{hex}}$  ratio versus temperature for  $\text{Li}_{0.50}\text{Ni}_{1.02}\text{O}_2$  ( $\Delta$ ),  $\text{Li}_{0.30}\text{Ni}_{1.02}\text{O}_2$  ( $\nabla$ ),  $\text{Li}_{0.50}\text{Ni}_{0.89}\text{Al}_{0.16}\text{O}_2$  ( $\blacksquare$ ) and  $\text{Li}_{0.30}\text{Ni}_{0.89}\text{Al}_{0.16}\text{O}_2$  ( $\bullet$ ). The  $a_{\text{hex}}$  and  $c_{\text{hex}}$  parameters were calculated from the X-ray diffraction patterns recorded *in situ* upon increasing temperature.